Available online at www.sciencedirect.com
ScienceDirect
International Journal of Heat and Mass Transfer 51 (2008) 1095–1103
International Journal of HEAT and MASS TRANSFER
www.elsevier.com/locate/ijhmt

Experimental analysis of the unit cell approach for two-phase flow dynamics in curved flow channels

D.M. Kirpalani [a,*], T. Patel [b], P. Mehrani [a], A. Macchi [b]

[a] Institute for Chemical Process and Environmental Technology, National Research Council of Canada, M-12 Montreal Road, Ottawa, ON, Canada K1A 0R6

[b] Department of Chemical Engineering, University of Ottawa, 161 Louis Pasteur Street, Ottawa, ON, Canada K1N 6N5

Received 6 November 2006; received in revised form 14 May 2007
Available online 14 August 2007

Abstract

Flow behavior of gas–liquid mixtures in thin channels has become increasingly important as a result of miniaturization of fluid and thermal systems. The present empirical study investigates the use of the unit cell or periodic boundary approach commonly used in two-phase flows. This work examines the flow patterns formed in small tube diameter (<3 mm) and curved geometry flow systems for air–water mixtures at standard conditions. Liquid and gas superficial velocities were varied from 0.1 to 7.0 (~±0.01) m/s and 0.03 to 14 (~±0.2) m/s for air and water respectively to determine the flow pattern formed in three geometries and dispersed bubble, plug, slug and annular flow patterns are reported using high-frame rate videography. Flow patterns formed were plotted on the generalized two-phase flow pattern map to interpret the effect of channel size and curvature on the flow regime boundaries. Relative to a straight a channel, it is shown that a 'C shaped' channel that causes a directional change in the flow induces chaotic advection and increases phase interaction to enhance gas bubble or liquid slug break-up thus altering the boundaries between the dispersed bubble and plug/slug flow regimes as well as between the annular and plug/slug flow regimes.
© 2007 Published by Elsevier Ltd.

Keywords: Mini-channel; Curved channel; Gas–liquid two phase flow; Flow mapping, mixing

1. Introduction

The recent emergence of micro-scale fluid, thermal and chemical systems has led to a renewed emphasis on the research of fluid flow behavior in small tube diameter flow systems such as ultra-compact heat exchangers, fuel cells, micro reactors, micro turbomachinery, micro thermal systems for a range of applications [1]. The advantages of such compact systems are the high surface area per unit volume, narrow residence time distribution, low installation cost, high efficiency and improved performance. Micro-fluidic technologies also address the demand for dissipating increasingly larger heat fluxes from energy sources. Thus, a great deal of research has been directed towards characterizing the flow morphology and transport phenomena with or without phase change in mini and micro-channels.

Flow regimes, established at a certain combination of the gas and liquid superficial velocities, depend upon fluid properties, flow channel dimensions, phase interaction and gravity, shear, inertia and surface tension forces. Transport phenomena in small diameter channels differ from those in conventional larger diameter channels primarily due to the differences in relative magnitudes of such forces. Surface forces and local rates of strain are dominant phenomena in small diameter channels that significantly reduce slip velocity rendering the flow characteristics independent of channel orientation with respect to gravity. The large aspect ratios (channel width to height = D/L) introduce relatively high pressure gradients at low velocities owing to high shear stress at the channel walls [2]. Unfortunately,

* Corresponding author. Tel.: +1 613 991 6958; fax: +1 613 991 2384.
E-mail address: deepak.kirpalani@nrc.ca (D.M. Kirpalani).

0017-9310/$ - see front matter © 2007 Published by Elsevier Ltd.
doi:10.1016/j.ijheatmasstransfer.2007.05.020

Nomenclature

D	channel internal diameter, m
Eo	Eotvos number=$(g(\rho_L - \rho_G)D^2)/\sigma$, –
F	$\sqrt{\rho_G/(\rho_L - \rho_G)}U_G/\sqrt{gD\cos\theta}$, –
g	gravitational constant, m/s^2
L	length of channel, m
P	pressure, Pa
R	radius of curvature as displayed in Fig. 2, m
T	$[(dP/dx)^S_L/((\rho_L - \rho_G)g\cos\theta)]^{0.5}$
U	superficial velocity, m/s
x	unit length, m
X	$[(dP/dx)^S_L/(dP/dx)^S_G]^{0.5}$

Greek symbols

σ	surface tension, N/m
θ	angle of inclination, °
ρ	density, kg/m^3

Subscripts

G	gas
L	liquid
S	superficial

there is no universal agreement that defines the limiting size of a small channel. Mehendale et al. [3] and Kandlikar [4] differentiated channels based on a hydraulic diameter where the delineation between small and conventional size channels is $D_H = 6$ mm for the former and $D_H = 3$ mm for the latter. Tripplett et al. [5] derived an expression using surface tension and gravitational forces and described a "characteristic length" as the delineation parameter for small channels and arrived at a diameter size of 2.75 mm for an air–water system at ambient temperature and pressure. Brauner and Moalem-Maron [6] defined an Eotvos number and proposed that a channel is considered small when surface force is significantly greater than gravitational force.

Flow regime boundaries in horizontal and inclined small or mini-channels have been the subject of research for many years. Suo and Griffith [7] investigated the flow patterns in horizontal channels of 1–1.6 mm in diameter. They identified slug, annular and dispersed bubble flow patterns and correlated flow regime transition boundaries based on the velocity of bubbles and average volumetric flow rates of the gas and the liquid phases. Taitel and Dukler [8] proposed a generalized dimensionless two-phase flow regime map based on momentum balances in each phase and the Kelvin–Helmhotz stability criterion for wave propagation. Barnea et al. [9] observed air–water flow morphology in horizontal channels of 4–12 mm in diameter and classified the flow patterns into dispersed bubble, annular, intermittent (plug and slug) and stratified. They suggested that the flow regime map reported by Taitel and Dukler was suitable for all flow regime boundaries except between stratified and intermittent flow. Damianides and Westwater [10] developed individual flow regime maps for air–water mixtures flowing through different tubes of 1–5 mm in diameter and observed dispersed bubble, intermittent, annular and dispersed flow patterns. Fukano et al. [11] investigated the flow patterns in tubes ($d = 1$–9 mm) for air–water mixtures and reported that surface tension forces become important for diameters less than 5 mm and that separated flow was not observed. Coleman and Garimella [12] studied the effect of tube diameter and shape on flow regime transition boundaries for air–water mixtures in tubes with hydraulic diameters of 1.3–5.5 mm They also confirmed that surface tension plays an important role in determining the flow patterns and transition boundaries for tube diameters less than 10 mm and found that the flow map developed by Taitel and Dukler [8] may not be valid. Tabatabai and Faghri [13] proposed a flow regime map, based on a force balances, that accounts for surface tension, shear and buoyancy forces and reported that the map was particularly effective in small diameter tubes of less than about 4 mm Overall, the contradictions in the findings [8–13] may be due to dissimilar geometries and test conditions.

There has been considerably less experimental work on the gas–liquid flow patterns in curved and serpentine channels with a 'C' shaped repeating unit. Wang et al. [14–16] studied the influence of a single return bend on the flow patterns of air–water mixture in 6.9, 4.95 and 3 mm circular horizontal channels and proposed flow regime maps. However, the effect of geometry on two-phase flow mixing and the resulting variation in flow regime boundaries has not yet been reported. Methods for developing computational models for two-phase flows in curved or 'C' shaped channels, such as serpentine flows in fuel cell applications and mini heat exchangers, have relied on a unit cell approach where periodic boundary conditions are affixed to a repeatable 'C' channel. This technique has been quite useful for single phase as well as reactive flows. However periodic boundaries do not account for phase transition and mixing encountered in two-phase mini flow systems. The extension of the periodic boundary modeling approaches needs to be validated at scale by a set of well defined experiments for small channels. Thus, the objectives of the present work are (1) Further investigate two-phase flow morphology and resulting regimes formed in curved channels and (2) Design an experimental procedure for evaluating the use of the unit-cell or periodic boundary modeling approach. Efforts were focused on developing two-phase flow regime maps for air–water mixtures in 1

and 3 mm diameter circular channels with a straight channel, a single curved 'C' channel and a serpentine or multiple 'C' shaped channels.

2. Experimental setup

Experiments were performed with air–water mixture flowing through horizontal channels. The schematic diagram of the experimental setup is shown in Fig. 1. Purified air with minimum impurities (laboratory grade) was used in the experiments. De-ionized (reverse osmosis) water was circulated using a gear pump through the flow channels from a 0.005 m^3 storage tank maintained at a temperature of 295 K and was dyed with methylene blue to provide a contrast between the two for analysis of collected images. Water flow meters with ranges of 0–1.6 $\times$ 10^{-6} m^3/

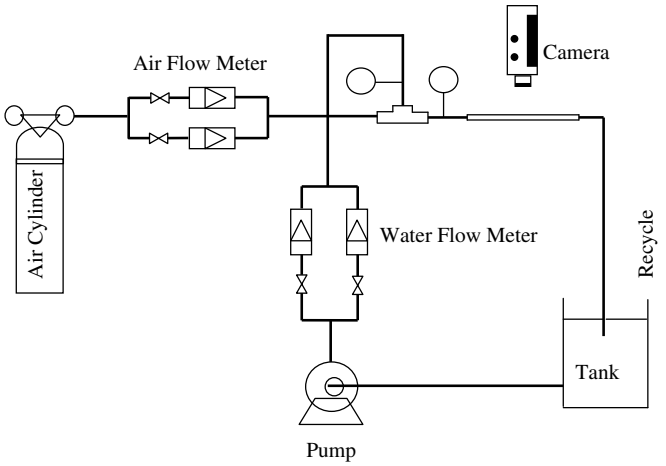

Fig. 1. Experimental set-up for thin channel two-phase flow studies.

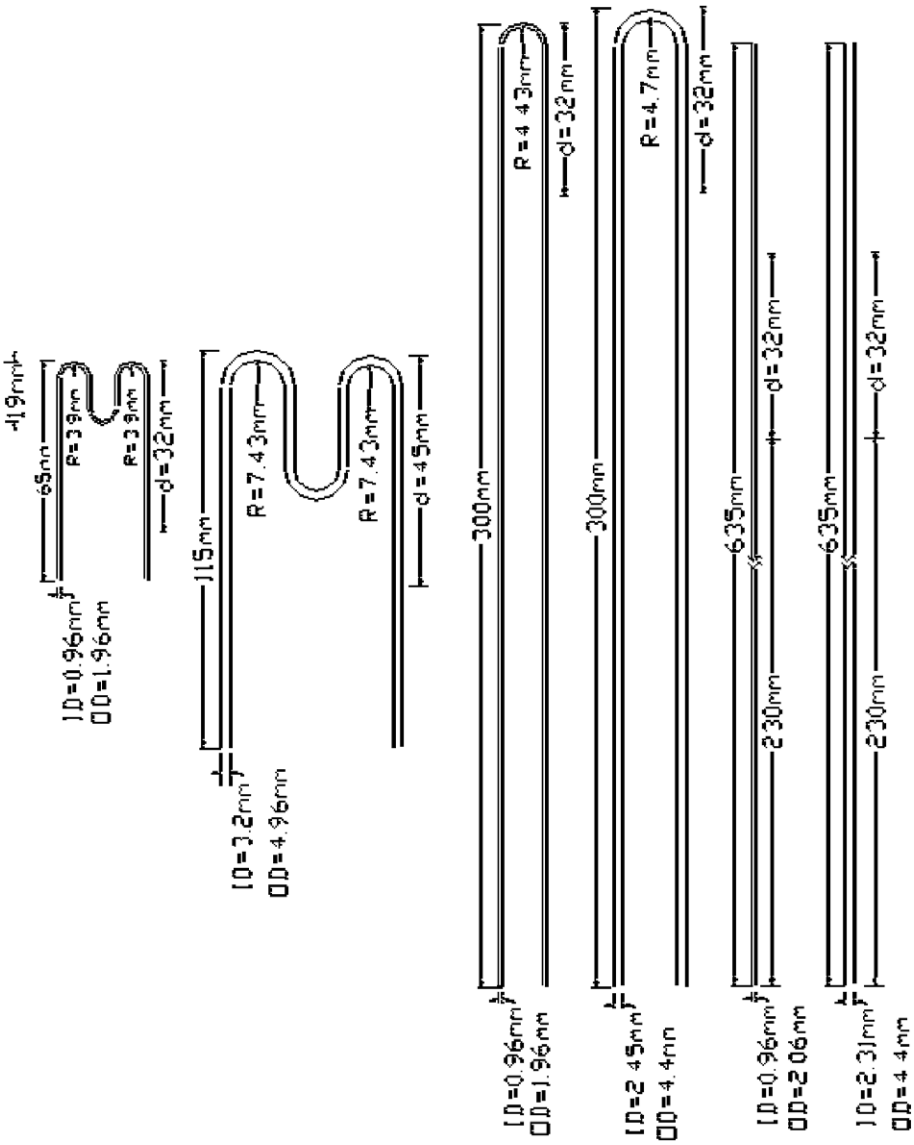

Fig. 2. Schematics of the 1 and 3 mm diameter glass channels used in the study.

s and 1.6×10^{-6}–3.3×10^{-5} m^3/s, and air flow meters with ranges of 0–8.3×10^{-6} m^3/s (STP) and $1.6 \times 10^{-6} - 6.7 \times 10^{-5}$ m^3/s (STP) were used to measure the volumetric flow rates of the two phases. Water and air were pre-mixed in a tee connector before the fluid mixture was introduced into the mini-channels. Also, pressure measurements were made near the entrance of the flow channels as shown in Fig. 1. A Redlake® CCD high-frame rate video camera with a 700 mm focal length lens, operating at 250 frames per second and a shutter speed of 1/2500, was used to capture images of the flow in the channels shown in Fig. 1. The images were recorded and further processed with imaging software for analysis. The video measurements were repeated at least three times in order to minimize any discrepancy in observations.

Six different geometric configurations for the small diameter channels were examined to characterize the flow patterns formed and evaluate the applicability of periodic boundary conditions or unit cell approach for multiphase flow modeling of a series of curved channels or serpentine-like channel. The channels, made of glass, having inner diameters of approximately 1 mm ($Eo = 0.134$) and 3 mm ($Eo = 1.2$). For the test conditions, the Eotvos number, $Eo \ll 1$, to ensure that surface forces strongly influence the flow patterns formed for the 1 mm channel and $Eo \sim 1$ with the 3 mm channel to study the effect of surface viscous and inertial forces. Fig. 2 illustrates the geometries studied in this work.

3. Results and discussion

3.1. Flow regime transitions

3.1.1. The 1 mm flow channel

Initial experiments were performed on 1 mm diameter flow channel. The liquid and gas superficial velocities were varied from 0.4 to 6.0 m/s and 0.04 to 12 m/s, respectively. For the straight channel length, only the plug and slug flow regimes were observed due to the prevalent surface forces that limit the formation of stratified, bubble and annular flow patterns. The observed flow patterns were also plotted on the flow regime map proposed by Taitel and Dukler [8] as shown in Fig. 3. The limitations of the Taitel and Dukler map are obvious, at low Eotvos numbers, and dispersed flow was predicted by the map while the observed flow pattern was slug flow. The gas flow rate was further increased during the experiments to obtain a dispersed bubble flow pattern. However, even at operating pressures of 200 kPa(g)., the dispersed flow pattern was not achieved. This may be due to the dominant surface forces in the mini-channel. It should be noted that surface forces, critical at low Eotvos numbers, are not accounted for in the Taitel and Dukler map. At high superficial gas velocities (>10 m/s), gas–liquid flows were relatively unsteady and slugging increased and high amplitude pressure fluctuations were observed but annular flows could not be obtained. Thus

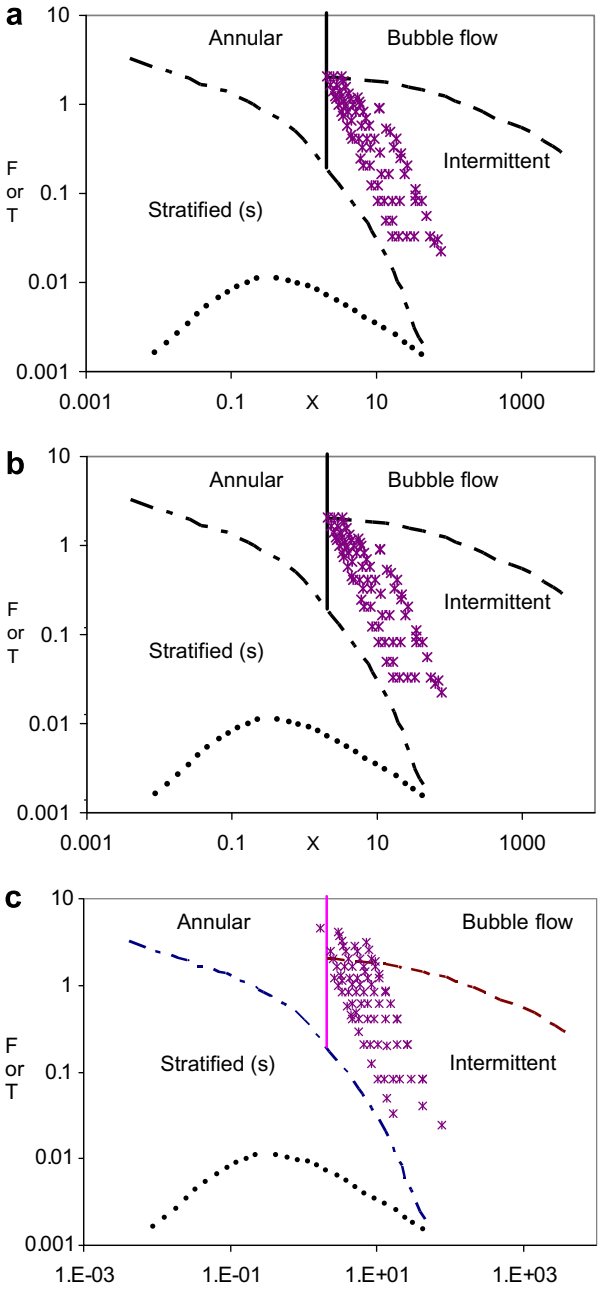

Fig. 3. Observed flow patterns for 1 mm diameter channels of different geometrical configurations mapped on the generalized two-phase flow map (Taitel and Dukler, 1976). (a) Straight channel, (b) 'C-shaped' curved channel and (c) Multiple 'C-shaped' curved serpentine channel.

the range of flow patterns reported by Triplett et al. [5] was not observed in this work.

Tabatabai and Faghri [13] performed a force balance on the phases and proposed a modified flow regime map that accounts for surface, shear and buoyancy forces. However, the model is not easily applicable because a priori knowledge of flow conditions is required for implementing the model. The addition of multiple 'C' channels or serpentine loops (1 'C'-channel to 3 'C' channels) shows limited gas bubble break-up and changes in flow pattern were not

observed over a wide range of conditions. The observed flow patterns were found to be limited to the intermittent or plug and slug flow patterns only. The limitation in determining the flow patterns formed can be attributed to viscous and surface forces and local rates of strain in small diameter channels used in this study. Periodic boundary modeling does not incorporate flow pattern information and the changes in flow patterns for repeating unit cells, such as 'C-shaped' channels is not accounted for in the modeling approach.

3.1.2. The 3 mm flow channel studies

Flow patterns formed in the ~3 mm internal diameter flow channel were studied over a wide range of liquid and gas superficial velocities. The gas and liquid superficial velocities were varied over the range of $0.1 < Q_L < 7.0$ m/s and 0.03 m/s $< Q_G < 14$ m/s, respectively. In this case, the dispersed bubble, plug, slug and annular flow patterns were obtained for the straight channel the single 'C' curved channel and the serpentine channel. However, stratified flow pattern was not observed in the specified operating range. Select images illustrating the flow patterns formed are shown in Fig. 4. Fig. 5 represents the observed flow patterns plotted on the flow regime map proposed by Taitel and Dukler [8]. Unlike the 1 mm diameter channels, the flow patterns formed are found to be in reasonable agreement with collected images from a straight channel. Also, unlike the 1 mm diameter flow straight channel flow, very few discrepancies exist (Fig. 5) in the flow pattern predictions. In a micro-channel, motion of a particle (bubble), equivalent in size to the channel, can be determined by the resulting force due to hydrodynamics and inertial effects [17]. As inertial forces and viscous forces, become more significant than in 1 mm channels, the liquid tends to move towards the channel wall forcing the onset of intermittent flow leading to enhanced phase interaction. This change in flow patterns, from annular to intermittent flow patterns, becomes increasingly prominent by the inclusion of single 'C' curves and multiple 'C' curves or serpentines in the channel geometry.

Fig. 6 illustrates the shift in flow regime boundaries by re-configuring the flow path with 'C' curves. The regime boundary shifts indicate the relative transition in flow patterns that are obtained by varying the flow geometry only. As shown, the transition from intermittent (or slug) regime to annular and dispersed bubble regimes occurs in serpentine channels at significantly lower superficial liquid velocities. From a hydrodynamic point of view, as fluid flows

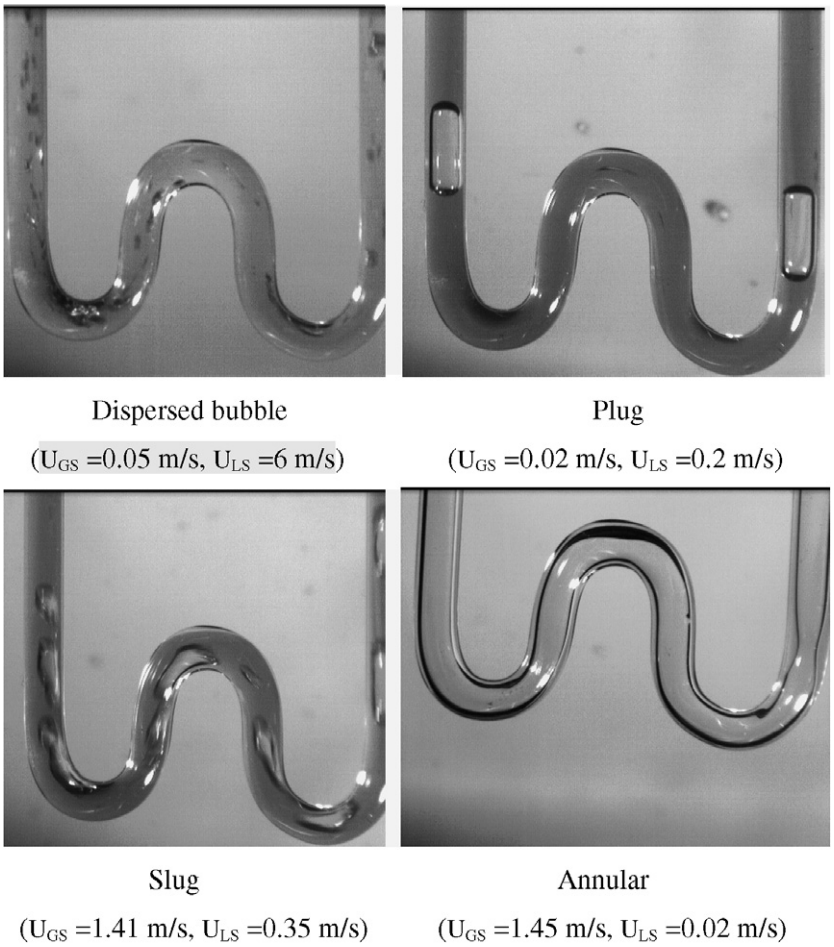

Fig. 4. Flow patterns observed in the 3 mm diameter serpentine channel at different liquid and gas superficial velocities.

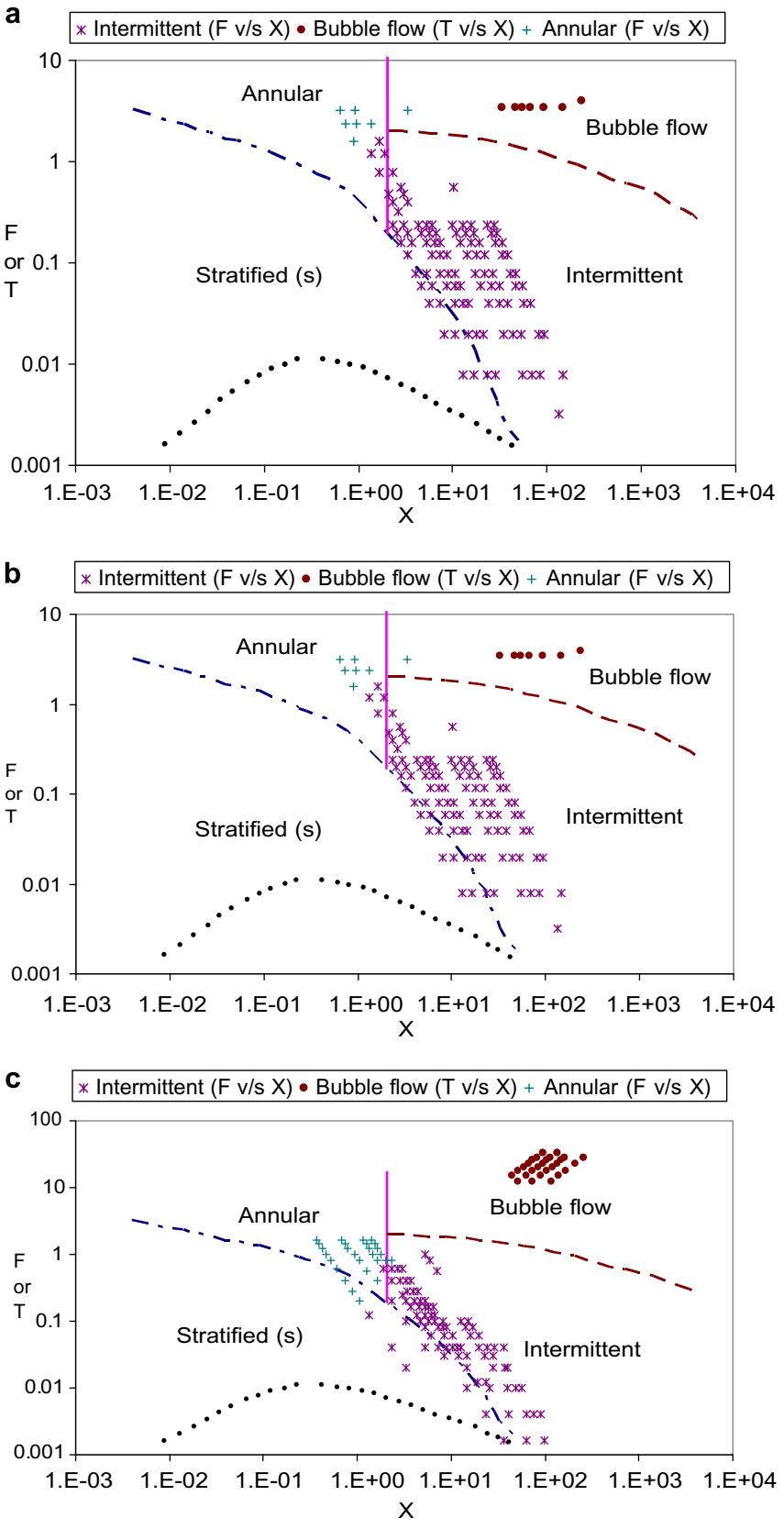

Fig. 5. Observed flow patterns for 3 mm diameter channels of different geometrical configurations mapped on the generalized two-phase flow map ([8]). (a) Straight channel, (b) 'C' curved channel and (c) multiple 'C' curved serpentine channel.

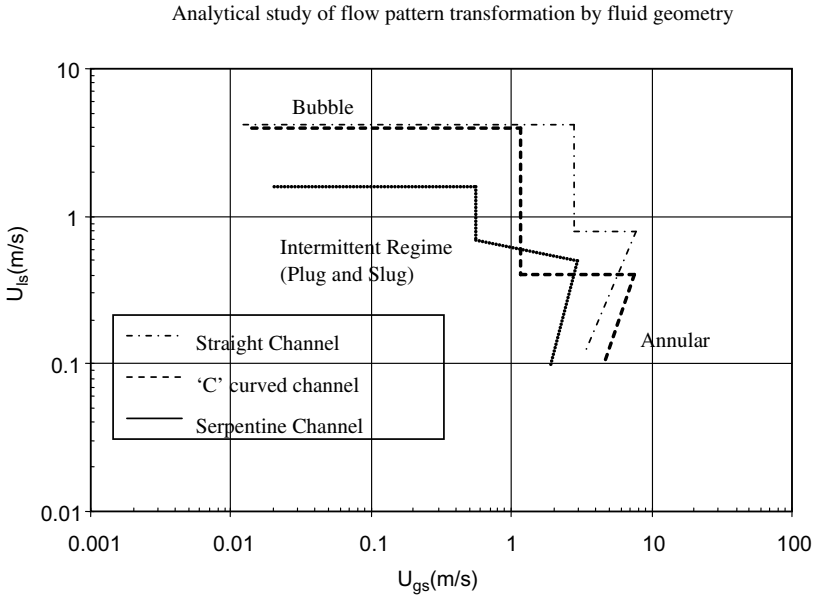

Fig. 6. Flow regime transition boundaries for different geometrical configurations of 3 mm channels.

through the curved channel, the centrifugal force drives the heavy fluid (water) with higher inertia as compared to gas which may result in breakage of gas bubbles. The presence of curved flow paths reduces the dispersed phase velocities and increases the probability of contact between bubbles that may coalesce or breakup depending on the bubble Weber number. The flow pattern formed is either annular flow at moderate gas superficial velocities and dispersed bubbles at high gas superficial velocities and pressure. Moreover, the curvature of channels increases the pressure gradient relative to an equivalent length of straight channel. The findings from this work also confirm that the transition from an intermittent to dispersed bubble flow occurs at lower liquid superficial velocities and the transition from intermittent to annular flow occurs at lower gas superficial velocities due to increased pressure gradient as previously reported by Coleman et al. [12].

The inclusion of curved channels tends to translate the flow patterns from intermittent flow to dispersed bubble or annular flow and flow patterns formed change by increasing the number of repeatable 'C' curves from a single 'C' curve channel to a multiple 'C' curves (or serpentine) in the fluid path. This flow pattern transition due to curvature provides an increase in pressure drop and mixing of phases and periodic boundary models may not be appropriate for the periodic albeit flow pattern changing multiphase geometry.

3.2. Dispersed phase break-up dynamics

3.2.1. Intermittent-dispersed bubble flow

The flow pattern changes over the length of the channel starting with the formation of large gas bubbles or slugs indicating, intermittent flow, that tend to break-up as they traveled through the bends of the curved channels, thus leading to dispersed bubble flow, was observed to be more predominant in serpentine channels and was found to be limited by gas slug length in the 3 mm diameter channel. Fig. 7 shows the break-up of a gas slug as it travels through the second C-curve bend of the 3 mm channel. In Frame 1, the highlighted large gas bubble travels through the first bend of the channel without any breakage. In the next image (Frame 2) and the second 'C' curve, the bubble elongates and finally breaks up (Frame 3). Further break-up of the gas bubble is not observed in the final straight length of the channel. This shows that the distortion of the gas–liquid interface, even at lower Reynolds numbers, illustrates that the twists in the flow through the serpentine channel generate strong secondary flows that provide significant stretching and eventual breakup of the bubbles. Although, this study assumes isothermal behavior of the fluids, irrespective of size, channel curvatures generate secondary flows in the channel cross plane that increase friction factors moderately and Nusselt numbers significantly [2].

For the serpentine channel, the threshold limit for initiating break-up of gas bubbles commences at low superficial liquid and gas velocities of 0.1 m/s and 1.03 m/s, respectively. At this flow condition, small gas pockets tend to break away from the wave of the large gas bubbles as shown in Fig. 7. At higher liquid velocities, the break-up of gas bubbles occurred at lower gas velocities indicating a critical ratio of inertial forces between the gas and the liquid for initiating bubble breakup in a specified curved geometry. The mechanism of bubble break-up due to curvature can be further extended from an inertial force ratio to include flow geometry by developing a two-phase dimensionless number, analogous to the Dean number, that accounts for secondary vortices and phase distribution and includes the straight lengths (L) between consecutive

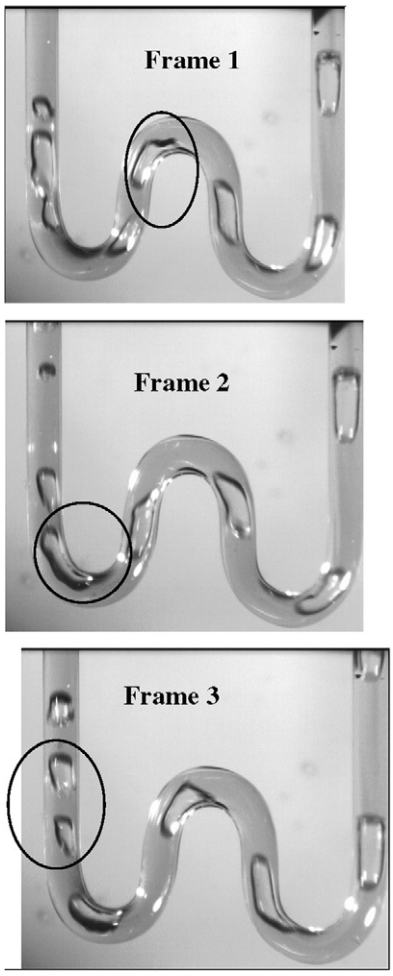

Fig. 7. High speed video frames showing break-up of large gas bubbles at low gas to liquid velocity ratios due to secondary vortices in the 3 mm serpentine channel.

curves. If the non-linear dimension between curves in the channel (L/D) that represents the straight length between curved flow paths is sufficiently long, then the original flow pattern has sufficient time to recover and the elongated large bubbles from the curved section may revert back to inlet bubble size. Alternately, small straight lengths between curves may not provide sufficient residence time in the straight channel leading to elongated bubbles that travel through the serpentine. The high local rates of strain due to the walls of the channel also contribute significantly towards limiting the breakup of gas bubbles in the 1 mm channels.

This passive phase mixing approach in serpentine mini-channels, that does not include the complexities of obstructions, can be used to obtain a phase re-distribution to dispersed bubbles. This may be suitable for improving mass transfer in thin channel applications that are limited since baffles or other mixing devices cannot be used. This study can be further investigated, particularly with multiple curvatures thin channel geometries to understand the irregular nature of break-up gas bubbles. In this study, the tracking of bubbles in smaller diameter channels (<1 mm) is limited due to the resolution of collected images and can be enhanced by using advanced diagnostic approaches such as local laser interferometry, neutron radiography and micro-particle image velocimetry can be used to study the gas–liquid interface, phase velocities and distribution.

3.2.2. Intermittent -slug flow

At relatively high gas and low liquid superficial velocities, liquid slugs are formed in a gas-continuous phase. Further evidence of enhanced mixing was obtained in the curved flow channels as liquid slugs flowed through the straight length of the channel and churn flow was induced when the slugs passes through the curved portions or flow reversal sections of the channels. This effect was more significant in the serpentine channel where the liquid slug passed through multiple 'C' geometrical curvatures as shown in Fig. 8. Visually, tangential flows are induced as

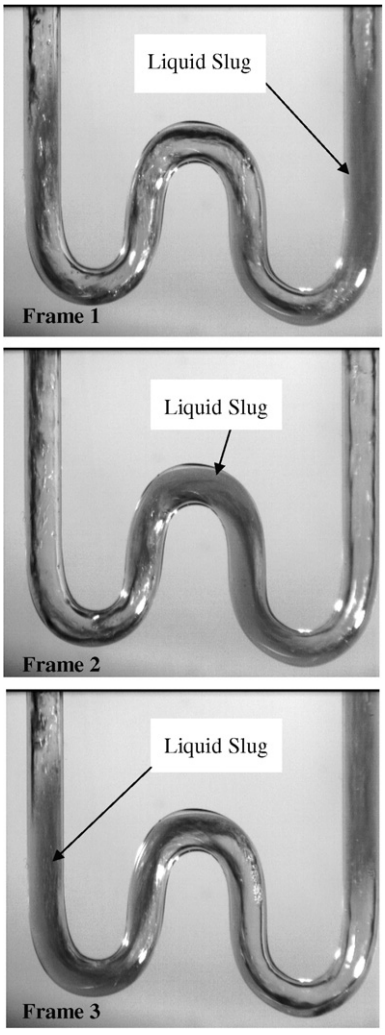

Fig. 8. High speed video frames showing break-up of liquid slugs occurring at high liquid flow rates in the 3 mm serpentine channel.

liquid slugs twist while passing through the curvatures in the serpentine channel. Secondary flows, formed in the curved profile, generated due to forced centrifugal motion, tend to drive the gas phase into the concave profile of the curved channel, while the heavier fluid or liquid moves to the convex part to slow down. This phenomenon generally leads to a transition from intermittent to annular flow.

4. Conclusion

An experimental assessment of two-phase flow behavior in thin channels (1 and 3 mm) with different geometrical configurations was performed with air–water mixtures. For the 1 mm diameter channel, in contrast to previous work, only plug or slug flow patterns were observed, irrespective of the change in liquid and gas flow rates. Surface forces acting on the slugs of liquid or large gas bubbles govern the flow behavior and changes in flow geometry had limited impact on the flow pattern formed. The generalized flow regime map of Taitel and Dukler [8] was also found to be limited in predicting the flow behavior for the 1 mm diameter channel.

For the 3 mm diameter channels, Taitel and Dukler's flow map was found to be in agreement for the straight channel. However, other geometrical configurations that include single and multiple curved 'C' bends, with limited recovery zones or straight lengths in between the bends, produced secondary flow patterns inducing gas and liquid slugs break-up. This led to flow regime changes and reduced the dependability of the flow map. This study showed that passive phase re-distribution, based on geometrical configurations, can be applied to thin channel two-phase flow devices to improve heat and mass transfer. Chaotic advection, required for improved phase interaction, depends on the three dimensionality of the flow field and is influenced by the inertial and viscous forces.

This work also confirms that flow modeling techniques, such as periodic boundary methods, that are applicable for single phase flows may be limited in curved two-phase flow applications due to the regime transitions that occur as a result of geometrical configurations. The flow distribution through the serpentine channel shows that the two-phase distribution changes with every 'C' bend in the channel and the geometrical profile of the channel significantly impacts the flow behavior. The changes in fluid flow behavior due to changes in flow path need to be addressed in flow maps and in two-phase flow simulations.

Acknowledgements

The authors acknowledge the financial support given by the Climate Change Technology and Innovation-HEIST fund for this work. The authors acknowledge the suggestions made by Prof. W. Minkowycz and other reviewers on the submitted paper.

References

[1] R. Shekarriz, Challenges in thermal systems miniaturization, Heat Transfer Eng. 21 (2000) 1–2.
[2] L. Wang, F. Liu, Forced convection in slightly curved microchannels, Int. J. Heat Mass Transfer 50 (2007) 881–896.
[3] S.S. Mahendale, A.M. Jacobi, R.K. Ahah, Fluid flow and heat transfer at micro- and meso-scales with application to heat exchanger design, Appl. Mech. Rev. 53 (2000) 175–193.
[4] S.G. Kandlikar, Fundamental issues related to flow boiling in minichannels and micro-channels, Exp. Therm. Fluid Sci. 26 (2002) 38–47.
[5] K.A. Triplett, S.M. Ghiaasiaan, S.I. Abdel-Khalik, D.L. Sadowski, Gas–liquid two phase flow in microchannels, Part I: Two-phase flow patterns, Int. J. Multiphase Flow 25 (1999) 377–394.
[6] N. Brauner, D. Moalem-Maron, Identification of the range of small diameter conduits, regarding two-phase flow pattern transition, Int. Commun. Heat Mass Transfer 19 (1992) 29–39.
[7] M. Suo, P. Griffith, Two-phase flow in capillary tubes, J. Basic Eng. 86 (1964) 576–582.
[8] Y. Taitel, A.E. Dukler, A model for predicting flow regime transition in horizontal and near horizontal gas liquid flow, AIChE J. 22 (1976) 47–55.
[9] D. Barnea, Y. Luninski, Y. Taitel, Flow pattern in horizontal and vertical two phase flow in small diameter pipes, Canadian J. Chem. Eng. 61 (1983) 617–620.
[10] C.A. Damianides, J.W. Westwater, Two-phase flow patterns in a compact heat exchanger and in small tubes, Proc. 2nd UK National Conf. Heat Transfer 19 (1988) 185–190.
[11] T. Fukano, A. Kariyasaki, Characteristics of gas–liquid two-phase flow in a capillary, Nucl. Eng. Des. 141 (1993) 59–68.
[12] J.W. Coleman, S. Garimella, Characterization of two-phase flow patterns in small diameter round and rectangular tubes, Int. J. Heat Mass Transfer 42 (1999) 2869–2881.
[13] A. Tabatabai, A. Faghri, A new two-phase flow map and transition boundary accounting for surface tension effects in horizontal miniature and micro tubes, J. Heat Transfer 123 (2001) 958–968.
[14] C. Wang, I.Y. Chen, Y. Yang, Y. Chang, Two-phase flow pattern in small diameter tubes with the presence of horizontal return bend, Int. J. Heat Mass Transfer 46 (2003) 2975–2981.
[15] C. Wang, I.Y. Chen, Y. Yang, Y. Chang, R. Hu, Influence of horizontal return bend on the two-phase flow pattern in small diameter tubes, Exp. Therm. Fluid Sci. 28 (2004) 145–152.
[16] C. Wang, I.Y. Chen, P. Huang, Two-phase slug flow across small diameter tubes with the presence of vertical return bend, Int. J. Heat Mass Transfer 48 (2005) 2342–2346.
[17] Y.F. Yap, J.C. Chai, T.N. Wong, N.T. Nguyen, K.C. Toh, H.Y. Zhang, Particle transport in microchannels, Numer. Heat Transfer Part B: Fundam 51 (2007) 141–157.